ELSEVIER

Contents lists available at ScienceDirect

Journal of the European Ceramic Society

journal homepage: www.elsevier.com/locate/jeurceramsoc





Understanding the depolarization temperature in $(Bi_{0.5}Na_{0.5})$ TiO_3 -based ferroelectrics

Zhongming Fan*, Sevag Momjian, Clive A. Randall

Materials Research Institute, Pennsylvania State University, University Park, PA 16802, USA

ARTICLE INFO

Keywords:
Bismuth sodium titanate
Depolarization temperature
Defect chemistry
Pyroelectric
In situ transmission electron microscopy

ABSTRACT

Depolarization temperature, or $T_{\rm d}$, in ferroelectric materials limits the high temperature operation regime as the long range dipolar ordering could not be maintained beyond $T_{\rm d}$ during zero field heating. Therefore, the control of $T_{\rm d}$ has been always drawing the attention of the ferroelectric/piezoelectric community. Some particular issues include: Which point defect is more responsible for the change of $T_{\rm d}$? What is the phase equilibrium as a function of $T_{\rm d}$? In this paper, our goal is to elaborate the correlation between $T_{\rm d}$ and defect chemistry in 85% (Bi_{0.5}Na_{0.5}) TiO₃-15% BaTiO₃ (BNT-15BT) ferroelectric ceramics. Various experimental tools are employed and cross referenced, including dielectric measurements, thermal stimulated depolarization current, impedance spectroscopy, scanning transmission electron microscopy and in-situ transmission electron microscopy. Collectively this study generates a more insightful understanding of $T_{\rm d}$ in BNT-based ferroelectrics.

1. Introduction

Some ferroelectric materials go through a depolarization temperature, T_d , which influences the nature of long range dipolar ordering. In normal ferroelectrics like BaTiO3, $T_{\rm d}$ is technically the Curie point [1]. In poled relaxor ferroelectrics like $Pb(Mg_{1/2}Nb_{2/3})O_3$, T_d occurs at a lower temperature than the maximum point of a dielectric curve, and is more associated with the freezing temperature - as determined via the Vogel-Fulcher dependence of the relaxation [2]. As suggested by its name, T_d is accompanied with a disruption of microsized ferroelectric domains, leading to a suppression of remanant polarization thereby a loss of piezoelectric responses. Conventionally, increasing $T_{\rm d}$ is of greater interest as a wider temperature window for operation is always favored in piezoelectric ceramics. Compositional design for the ferroelectric transition behavior can be guided by crystal chemical trends such as dependences in perovskite crystal structures and tungsten bronze structures on Goldschmidt tolerance factors. As an example, a linear relation between Curie temperature and tolerance factor was identified in Bi-based solid solutions [3]. Other methods to influence the ferroic displacive phase transitions can involve point defects concentration. For instance, annealing BaTiO3 in reducing atmosphere was found to defer the Curie temperature, which could be attributed to either the oxygen vacancies or the electronic charge that are created during the annealing treatment [4].

The correlation between $T_{\rm d}$ and defect chemistry can be quite complexed in (Bi_{0.5}Na_{0.5})TiO₃ (BNT) system owing to a wide variety of degrees of freedom. Due to votility, Bi and Na vacancies must be taken into account in the BNT system. In the meantime, oxygen vacancies should also be considered as they ionically compensate for the negative charges associated with the cation vacancies (throughout this paper, Kröger-Vink notations are employed in the defect reaction equations. "V" stands for vacancy, "×" "•" and "d" indicates neutral, positive, and negative charge, respectively),

$$2Bi_{Bi}^{\times} + 3O_O^{\times} \xrightarrow{BNT} 2V_{Bi}^{\prime\prime} + 3V_O^{\bullet\bullet} + \alpha(Bi_2O_3)$$
 (1)

$$2Na_{Na}^{\times} + O_O^{\times} \xrightarrow{BNT} 2V_{Na}^{\prime} + V_O^{\bullet \bullet} + \alpha(Na_2O)$$
 (2)

Therefore, a natural difficulty is to discern whether it is the cation vacancy or oxygen vacancy that controls $T_{\rm d}$. Genernally, oxygen vacancy or oxygen vacancy — cation vacancy associated defect dipole distributions are known to have substantial impacts on the domain switchability under electric field [5]. However, whether the oxygen vacancy population can "stablilize" the ferroelectric ordering against thermal energy remains an open question. There is compelling evidence that quenching from very high temperatures can increase the $T_{\rm d}$ in BNT-based relaxor ferroelectrics as noted by several research groups [6, 7]. One possible explanation is that quenching circumvents the super-oxidation process and thereby leaves more ionically oxygen

E-mail address: zbf5066@psu.edu (Z. Fan).

^{*} Corresponding author.

vacancies in the ceramics. However, quenching produces chemical gradients and associated residual stresses, which is another possible factor affecting $T_{\rm d}$ [8]. Thus, elucidation of the $T_{\rm d}$ — defect chemistry relation requires more systematic investigation. In this paper, the base composition we chose to study this issue is $0.85({\rm Bi}_{0.5}{\rm Na}_{0.5}){\rm TiO}_3$ — $0.15{\rm BaTiO}_3$ (BNT-15BT).

2. Experimental

The BNT-15BT ceramics were fabricated using conventional solid state reaction method, with starting powders of Bi₂O₃ (Sigma Aldrich, >99.9%), Na₂CO₃ (Alfa Aesar, >99.95%), TiO₂ (Sigma Aldrich, >99.9%), BaCO₃ (Alfa Aesar, >99.8%), and Ta₂O₅ (Alfa Aesar, >99.99%) weighed according to specific compositions. The mixed powders (batch size of ~ 20 g) were ball milled in ethanol for 24 h, both before and after being calcined. For all the investigated compositions, the calcination and sintering were carried out at 900 °C and 1200 °C, respectively, for 2 h. The as-sintered pellets were polished to ~ 1 mm in thickness before platinum electrodes were sputtered. The impedance spectroscopy was obtained by a computer-controlled furnace with a Solartron ModuLab XM impedance analyzer from 0.1 Hz to 1 MHz. Dielectric properties were measured using LCR meter (4284 A, Agilent Technologies). Thermally stimulated depolarization current (TSDC) data were collected by a pA meter (4140B, Hewlett Packard). The grain size analysis was carried out based on the Scanning Electron Microscopy micrographs (Verios G4, Thermal Scientific) that were taken from the thermally etched polished surfaces. The Transmission Electron Microscopy (TEM) was performed on Talos F200X (Thermal Fisher Scientific). The secondary phases were identified through the quantification of the EDS spectrum acquired using SuperX EDX detector. In situ TEM was conducted on a Protochip heating holder.

3. Results and discussion

The dielectric permitivity of stoichiometric undoped BNT-15BT exhibits very little frequency dispersion from room temperature till it undergoes a steep rise above 210 °C (Fig. 1a). Such dielectric characteristics are common to the BNT-BT solid solutions and unambiguously represent a transition to the *P4mm* normal ferroelectric phase in BNT-15BT [9]. The presence of micron-sized ferroelectric domains is indicated by the electron diffraction pattern taken at ambient temperature, which reveals the splitting of diffraction spots along < 110 > direction

(perpendicular to 90° domain walls, highlighted with a red circle in Fig. 1b). Following that steep rise, a broad dispersive peak is seen in the dielectric curve, which suggests the nature of the polarization being that of a relaxor ferroelectric phase. Correspondingly, the diffraction splitting vanishes when the long-range ferroelectric order is disrupted at elevated temperature (Fig. 1c). It should be noted that the high temperature electron diffraction pattern does not contain any superlattice reflections. This means that the relaxor phase in BNT-15BT may also feature *P4mm* symmetry, rather than a octahedral tilted *P4bm* with $\frac{1}{2}$ {ooe} superlattice relections which would have been observed at the position given by the green circle in Fig. 1c [9]. Thus, the thermal depolarization process in BNT-15BT is essentially a ferroelectric to relaxor phase transition without a change in crystal structure and a coupled tilt transition.

A common way to decrease the T_d in ferroelectric materials is to dope with aliovalent cations, doping La to Pb(Zr,Ti)O3 making it PLZT is a well explored example [10]. In this study, Ta⁵⁺ is chosen as a donor dopant on the Ti^{4+} site in BNT-15BT. With up to 2% Ta^{5+} doping, T_d has been decreased by more than 170 °C (Fig. 2a). Note that the T_d in this plot are all measured from poled samples, otherwise the BNT-15BT-2% Ta which is already relaxor phase at room temperature does not "display" a T_d . The T_d drop as a function of Ta⁵⁺ doping is nearly a linear line at low doping concentration, but there is a deviation when the doping amount increases. It is important to ask why is $T_{\rm d}$ drop accelerated at high doping levels? To answer this question, we will need to carefully consider the compensation mechanism for the donor doping. In general, the positive charge of the donor dopant can be compensated by either electron (Eq. 3) or cation vacancies. In Nb doped BaTiO3, the compensation by electron occurs when the doping concentration is very low [11], while the compensation mechanism switches to cation vacancy in more heavily doped cases [12].

$$Ta_{2}O_{5} \xrightarrow{BNT} 2Ta_{Ti}^{\bullet} + 2e' + 5O_{O}^{\times}$$
 (3)

In all of our doped samples, the conductivity is not seen to be enhanced (Fig. 2b), suggesting it is not an electronic compensation mechanism. Therefore, we consider the ionic compensation, also discern which of the cation vacancies is created, Bi vacancies (Eq. 4), Na vacancies (Eq. 5), or Ba/Ti vacancies (Eq. 6),

$$3Ta_2O_5 + 2Bi_{Bi}^{\times} \xrightarrow{BNT-15BT} 6Ta_{Ti}^{\bullet} + 2V_{Bi}^{\prime\prime} + 12O_O^{\times} + a(Bi_2O_3) \tag{4} \label{eq:4}$$

$$Ta_{2}O_{5} + 2Na_{Na}^{\times} \xrightarrow{BNT-15BT} 2Ta_{Ti}^{\bullet} + 2V_{Na}^{'} + 4O_{O}^{\times} + a(Na_{2}O)$$
 (5)

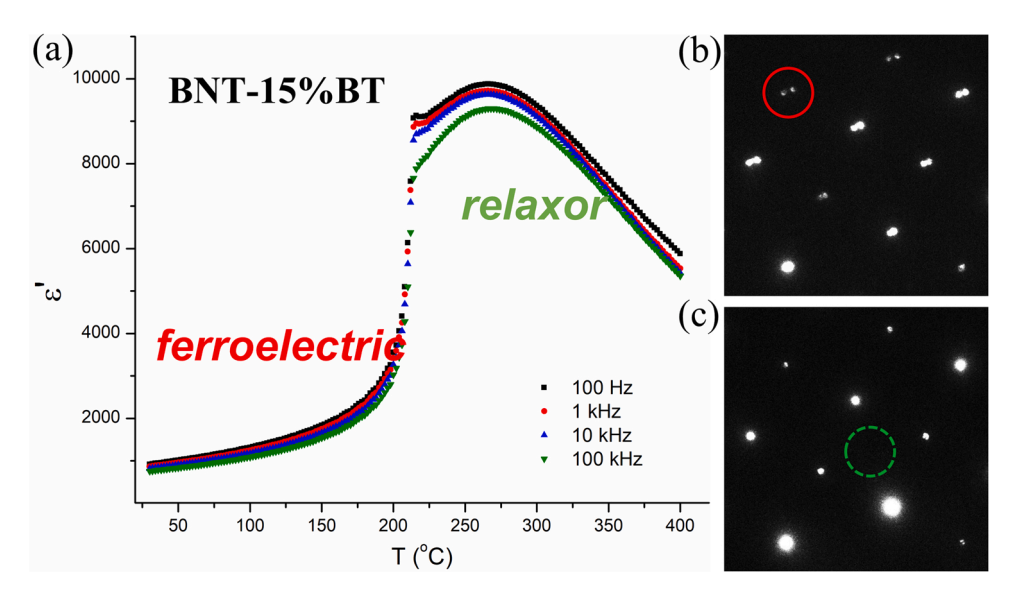


Fig. 1. (a) Dielectric constant as a function of temperature in BNT-15%BT ceramic. (b) Electron diffraction pattern from the low temperature ferroelectric phase with diffraction spot splitting indicative of displacive twins. (c) Electron diffraction pattern from the high temperature relaxor phase.

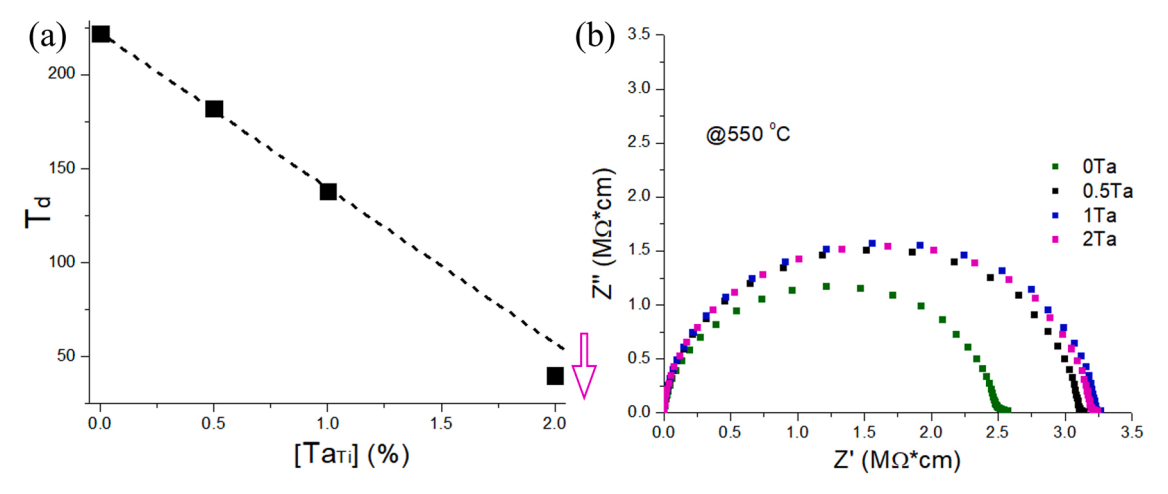


Fig. 2. (a) T_d drop in BNT-15BT with Ta^{5+} doping, the pink arrow indicates how the trend diviates from the linear relation. (b) Impedance spectroscopy from the Ta^{5+} doped BNT-15BT ceramics.

$$4Ta_{2}O_{5} + 2Ba_{Ba}^{\times} + Ti_{Ti}^{\times} \xrightarrow{BNT-15BT} 8Ta_{Ti}^{\bullet} + 2V_{Ba}^{\prime} + V_{Ti}^{\prime\prime\prime} + 16O_{O}^{\times} + Ba_{2}TiO_{4}$$
(6)

Technically, Ba/Ti vacancies can be ruled out first, since no Ba/Ti rich secondary phase is observed in the BNT-15BT-2%Ta after a TEM inspection. On the other hand, Bi and Na are both volatile species, hence the formation of their vacancies should not be ruled out despite the "single phase" observation. From Fig. 2a we have learnt that the cation vacancy generated with the donor doping is likely to decrease T_d too, so Bi deficiency compositional designs are introduced to BNT-15BT-1%Ta $(T_{\rm d} \sim 140\,^{\circ}{\rm C})$ to test if Bi vacancy increases or decreases $T_{\rm d}$. Fig. 3a shows that T_d does increase with Bi deficiency and it almost saturates when the deficiency is greater than 5%. Such saturation implies that the solubility limit of Bi vacancy is reached, meanwhile a Ti-rich secondary phase Ba₆Ti₁₇O₄₀ is found (Fig. 3b). On the other hand, one of the author's previous studies has concluded that the introduction of Na deficiency leads to the decrease of T_d in BNT-20BT ferroelectrics [13]. Thus, the compensation mechanism for the donor doping could be via the Na vacancies (Eq. 5).

According to Eq. (1), oxygen vacancies are also generated in association with Bi vacancies. Therefore, an alternative interpretation of Fig. 3a can be, $T_{\rm d}$ is increased because of oxygen vacancies instead of Bi vacancies. Indeed, with introducing Bi deficiency, ionic conduction is

also enhanced as determined from impedance spectroscopy methods. Stoichiometric BNT-15BT-1%Ta shows one symmetric peak in its electric modulus spectroscopy data (Fig. 4a). The activation energy associated with this peak is about 1.6 eV (Fig. 4b), close to the half band gap, suggesting a predominantly electronic conduction [14]. With Bi deficiency up to 1.6%, the modulus spectroscopy data still shows a singe symmetric peak, with the peak position barely changed (Fig. 4a). It means that the ionic conduction is not yet developed despite the fact that there should have been lots of oxygen vacancies in the material according to Eq. (1). The explanation could be that the $V_{Bi}^{\prime\prime}-V_{O}^{\bullet\bullet\bullet}$ defect association is so strong in BNT-15BT that it prevents the oxygen vacancies from long range migration. With 3.2% Bi deficiency, the modulus peak shifts to a higher frequency and a shoulder is found at even higher frequency (Fig. 4a). We have demonstrated in a previous publication that such two peaks in modulus originates from the mixed electronic-ionic conduction and can be readily seperated by the mixed conduction equivalent circuit (Fig. 4b,c) [15]. By further increasing the Bi deficiency, the modulus spectroscopy again shows only one symmetric peak, of which the activation energy is ~ 0.41 eV (Fig. 4c), a typical value for the ionic conduction in BNT-based ceramics [15]. So, it is therefore verified that the conductivity mechanism changes from predominantly electronic to mixed electronic/ionic to predominantly ionic as the Bi deficiency increases.

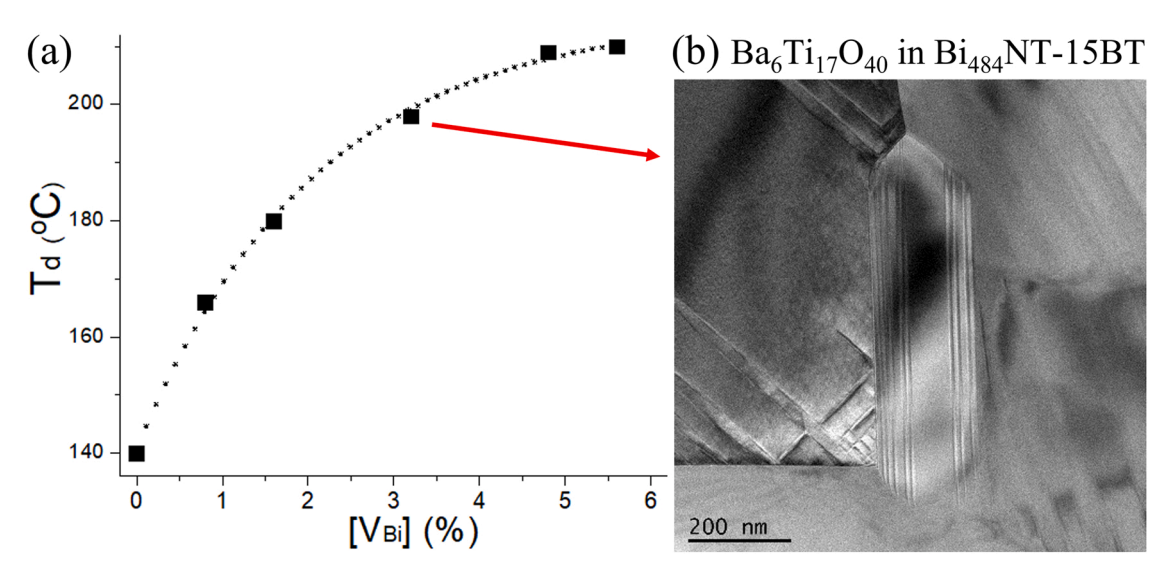


Fig. 3. (a) $T_{\rm d}$ rise with Bi deficiency in BNT-15BT-1%Ta. (b) Ti-rich secondary phase in Bi₄₈₄NT-15BT-1%Ta.

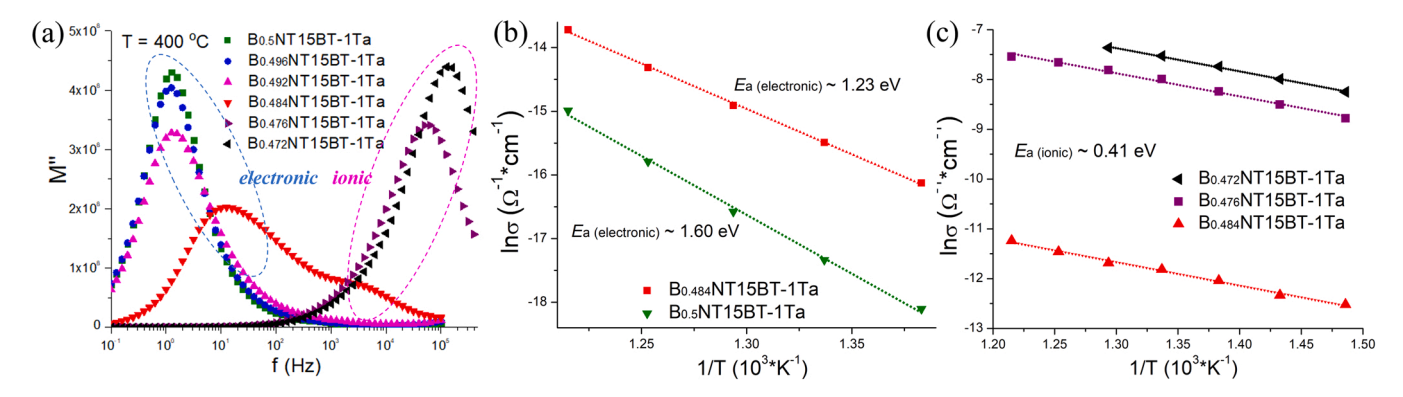


Fig. 4. (a) Electric modulas spectroscopy in BNT-15BT-1%Ta ceramics with different Bi deficiency. (b) Arrhenius plot for the electronic conductivity in the samples featuring mixed electronic/ionic conduction or predominantly electronic conduction. (c) Arrhenius plot for the ionic conductivity in the samples featuring predominantly ionic conduction or mixed electronic/ionic conduction.

The above observations still leave the question on whether the oxygen vacancy concentration is responsible for the rise of T_d ? In principle, if the rise of T_d is due to oxygen vacancies, sintering in an atomosphere with higher oxygen partial pressure should decrease $T_{\rm d}$, relative to the air sintered case. In fact, we will show that it is not always true and the correlation is a very complexed question (Fig. 5). When sintered in O_2 , the $T_{\rm d}$ of undoped BNT-15BT is lower than the air sintered sample. However, the $T_{\rm d}$ of BNT-15BT-0.5%Ta is maintained after the sintering atmosphere is switched from air to O2. More interestingly, the O2 sintered BNT-15BT-1%Ta even possesses a higher $T_{\rm d}$. In BNT-15BT-2%Ta, $T_{\rm d}$ is also increased, but by a larger amount. Subsequently, the samples with Bi deficiency combining with that 2%Ta doping are assessed. With 1.6% Bi deficiency, $T_{\rm d}$ is found to be invariant again. With 3.2% Bi deficiency, a lower T_d is seen in the O_2 sintered sample, like the situation in undoped BNT-15BT. Since O_2 is able to raise T_d or maintain T_d in particular compositions while lower T_d in others, we believe that the oxygen vacancy concentration may not play the most critical role in the $T_{\rm d}$ manipulation. We have learnt that the only type of point defect in BNT-15BT that can increase T_d is Bi vacancy.

$$3Ta_2O_5 + 2Bi_{Ri}^{\times} + O_2 \xrightarrow{BNT} 6Ta_{Ti}^{\bullet} + 2V_{Ri}^{\prime\prime} + 14O_0^{\times} + a(Bi_2O_3)$$
 (7)

So, the compensation mechanism for the donor doping might change from the generation of Na vacancies to Bi vacancies (Eq. 7) when sintered in O_2 , and this in turn results in a higher T_d . On the other hand, in those samples where the charge balance has been naturally satisfied between the existing $[Ta_{Ti}^{\bullet}]$ and $[V_{Bi}^{\prime}]$, the defect chemistry is not affected by air or O_2 sintering. We would like to point out that we do not

completely rule out the possibility for any correlation between oxygen vacancy and the T_d shift, as O_2 sintering does decrease the T_d in other compositions in which Bi vacancies are the dominant defects. For example, in B_{0.484}NT-15BT-1%Ta, the ionic conductivity is significantly suppressed by the O2 sintering, manifested by the disappearance of the higher frequency shoulder in the modulus peak (Fig. 6a). Here the T_d is reduced from \sim 198 °C (air sintered) to \sim 174 °C (O2 sintered). However, it is noticed that another defect that could account for this phenomenon. In O2 sintered B0.484NT-15BT-1%Ta, a Ba-rich secondary phase, Ba₂TiO₄, is discovered at the triple junction (Fig. 6b), which indicates that the major phase contains less Ba content. It is known that T_d monotonically decreases with Ba content as the composition approaches the morphotropic phase boundary. Therefore, the presence of Ba-rich secondary phase could tentatively explain for the T_d decrease in those O₂ sintered compositions. We also observed that the grain size reduces from $2.12 \pm 0.39 \, \mu m$ when sintered in air to $1.33 \pm 0.24 \, \mu m$ when sintered in O_2 (Fig. 6c,d) [16]. However, such a \sim 40% decrease might be too small to account for the > 20 °C $T_{\rm d}$ shift, considering the reported $50~^{\circ}$ C $T_{\rm d}$ deferral corresponding to a seventeen times grain growth in a very similar material [17].

In contrast to $\rm O_2$ sintering which leads to inconsistent shifts of $T_{\rm d}$, annealing the air sintered samples in reducing atmosphere consistently increases the $T_{\rm d}$ (Fig. 5). The annealing is conducted in Ar at 1150 °C for 3 h. A TEM study reveals a Ti-rich secondary phase, BaTi₄O₉, being generated under the Ar annealing (Fig. 7a). There is no doubt that the Ar annealing creates oxygen vacancies, and along with the Ti-rich secondary phase observations the generation of Bi vacancies is also implied.

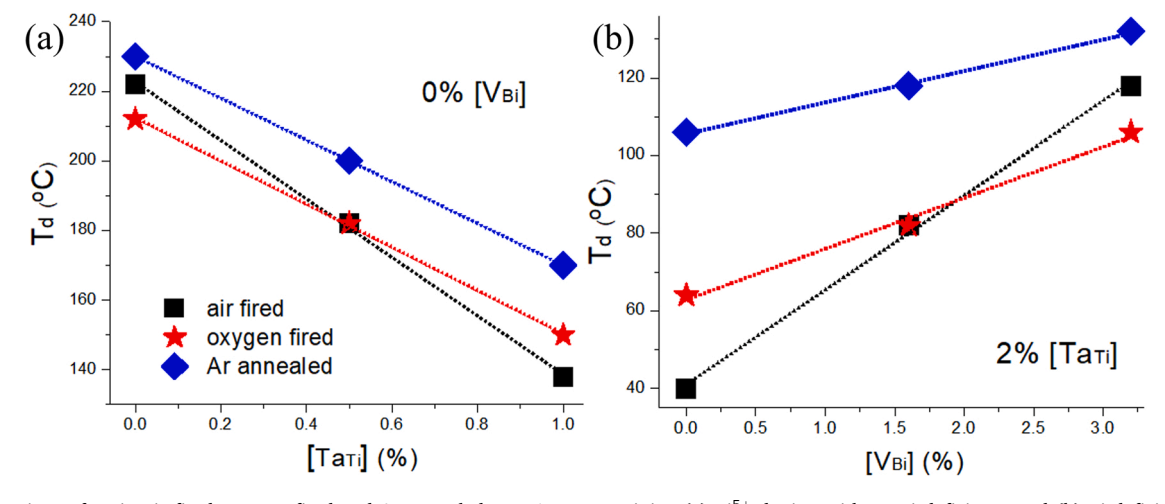


Fig. 5. Comparison of T_d in air fired, oxygen fired and Ar annealed BNT-15BT containing (a) Ti^{5+} doping with no Bi deficiency and (b) Bi deficiency with 2% Ta^{5+} doping.

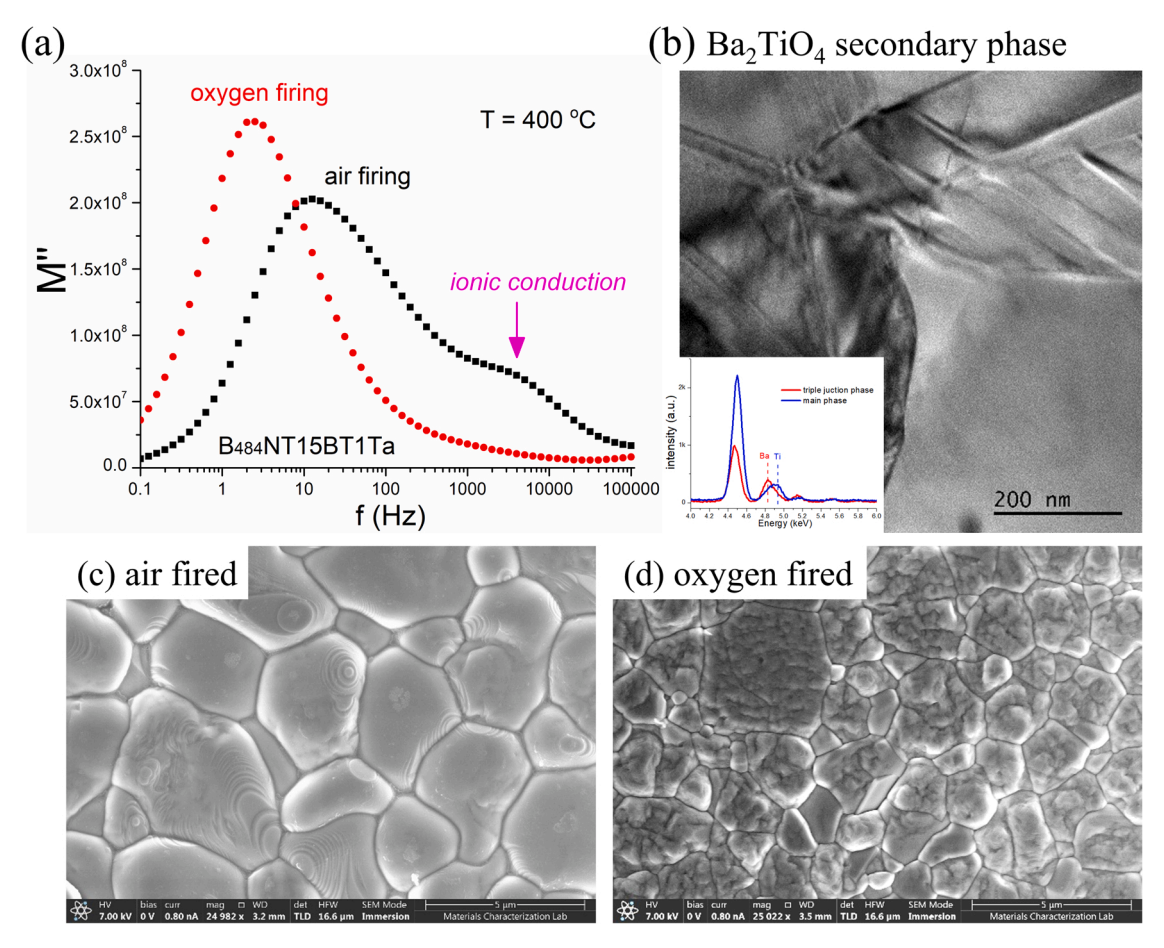


Fig. 6. (a) Electric modulas spectroscopy in $B_{484}NT15BT-1\%Ta$ fired in air and oxygen. (b) Ba rich secondary phase in oxygen fired $B_{0.484}NT15BT-1\%Ta$. The representative grain morphologies of the air and oxygen fired samples are shown in (c) and (d), respectively.

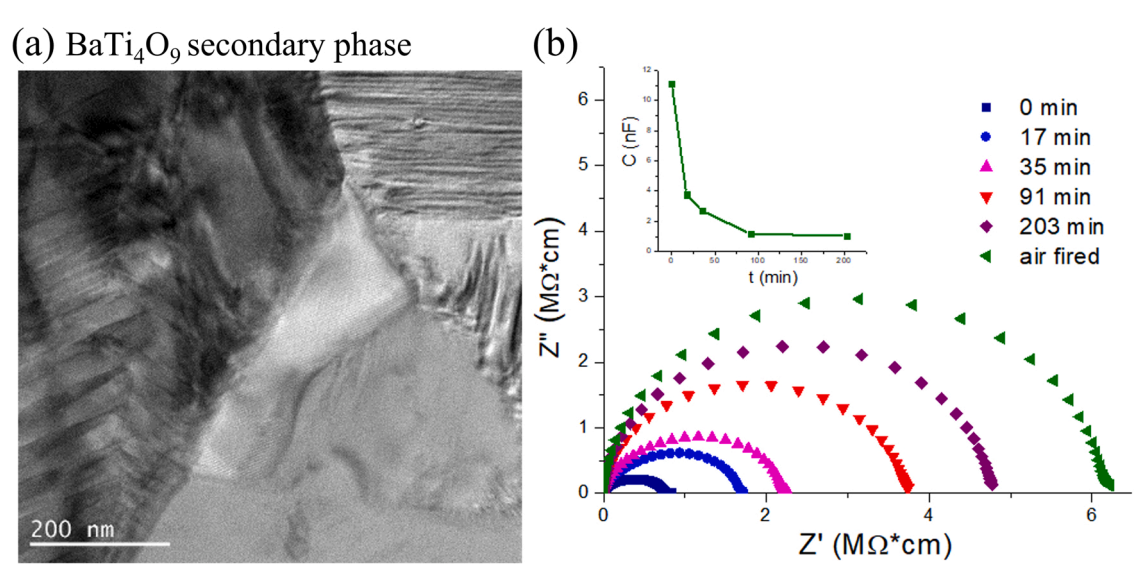


Fig. 7. (a) Ti rich secondary phase in BNT-15BT-1%Ta annealed in Ar at $1150\,^{\circ}$ C for 3 hrs. (b) The evolution of impedance and the associated capacitance while reoxidizing the Ar annealed sample in air at $450\,^{\circ}$ C.

Therefore, noting to whether Bi vacancy or oxygen vacancy causes the $T_{\rm d}$ rise becomes a necessary question again. So here we reoxidized the Ar annealed sample in air at 450 °C and tracked the evolution of conductivity (Fig. 7b). Initially, two semicircles are present in the impedance spectra. Presumably, the high frequency semicircle represents the reduced phase and low frequency one originates from the reoxidized

phase (reoxidation has begun before the temperature reaches 450 °C). Kept at 450 °C in air, the sample's conductivity continues to reduce. Specifically, the reoxidized phase gradually dominates over the reduced phase in volume fraction (Fig. 7b, inset), as suggested by the reducing capacitance over time. After 200-minute-reoxidation, the resistance of the sample almost recovers to the air sintered situation. However, the $T_{\rm d}$

does not "recover" at all. Accordingly, it is deduced that it is the Bi vacancies rather than the oxygen vacancy that are responsible for the $T_{\rm d}$ shift.

So far, all the T_d noted in this paper are determined to be coinciding with the position of the bump in temperature dependent dielectric loss curves in poled samples. Here we consider an alternative way to investigate details of the depolarization through the pyroelectric current as measured in a modified Byer and Roundy set up where the poled state is heated and the depolarization currents are monitored [18]. The data identifies multiple depolarization peaks in a BNT-15BT-2%Ta ceramic after annealed in Ar at relatively lower temperature for extended time (Fig. 8a). Since we have deduced that it is Bi vacancies that are responsible for the T_d rise, the distinguishable T_d s are likely the consequence of inhomogeneous Bi vacancy distributions within the microstructure. In fact, the multiple T_d can be clearly revealed by the dielectric loss curve from a poled sample too when considered under closer inspection. Upon heating, three bumps occurs one after another in the tanô data (Fig. 8c), matching up with the three pyroelectric peaks. If the heating ramp is terminated after the first bump just develops and then subsequently cooled back to room temperature rapidly, the first bump is "cleaned" and depolarized. Under a succesive heating up we only reveal the second and the third bumps. Similarly, after the first two bumps are both "depolarized", the third bump remains in the successive cooling and heating run. However, once all three bumps are "depolarized", a "bump" is still present in the dielectric loss curve, while it is such a broad one that renders the deconvolution of the stepwise depolarization process, if any, no longer easy. Fortunately, we found that TSDC can be very sensitive to those details even in the unpoled state. A "blank" TSDC is ran on the same sample in its unpoled (as-electroded) state. Three peaks are clearly resolved (Fig. 8d), which verifies that the ferroelectric ordering in the unpoled state is depolarized stepwisely as well.

It was also noticed that the measurement of T_d in poled samples is not subject to dielectric aging, while the temporally varying dielectric response can perturb the T_d determination in unpoled samples. For example, the $T_{\rm d}$ of stoichiometric BNT-15BT-1%Ta, measured in poled sample, is ~ 140 °C (Fig. 9a). However, the dielectric property of the unpoled sample is found to be very different depending on when it is measured. If the measurement is done as soon as possible after sintering/ annealing or in a queched sample, the dielectric curve exhibits the shape resembling that of a material being relaxor at room temperature (e.g. BNT-15BT-2%Ta). In comparison, if the measurement is done after a certain period of ambient temperature aging, the dielectric curve changes dramatically to a ferroelectric-like one (Fig. 9a), from which $T_{\rm d}$ can be directly read. Note that the evolution of the dielectric curve from a relaxor-like one to a ferroelectric-like one is continuous during aging, so, the $T_{\rm d}$ varies with aging time: later the measurement, higher the $T_{\rm d}$. However, the dielectric property in poled state, including T_d , is

independent upon when to measure it.

The evidence for the aging induced relaxor to ferroelectric transition can be found not only in dielectric measurement. Upon the initial electric field application, the polarization in the quenched sample sees an abrupt jump (Fig. 9b), which suggests a relaxor to ferroelectric phase transition induced under a certain field. Nevertheless, the polarization is built up more gradually during the initial poling in the aged state, which implies a normal domain switching process. Except for the intial poling section, the P-E loops from both states are completely overlapping. It means that a regular poling has induced an identical normal ferroelectric phase, which also corroborates the invariable $T_{\rm d}$ in poled sample. In addition to P-E loops, we also employed the "blank" TSDC to contrast the aged and quenched states. Both aged and quenched states display the pyroelectric peak in the "blank" TSDC, while that in the quenched state is apparently weaker (Fig. 9c). Although the dielectric curve appears to be relaxor-like, quenched BNT-15BT-1%Ta is actually not a pure relaxor phase, otherwise "blank" TSDC should never be able to detect the pyroelectric current, for instance, the $B_{0.484}NT-15BT-2\%Ta$ whose T_d is

The ferroelectric domain morphologies are directly visualized via in situ TEM. At ambient temperature, the aged BNT-15BT-1%Ta specimen shows a lamellar-shaped long-range ferroelectric domain configuration (Fig. 10a). Once the specimen is heated exceeding T_d , the lamellar domains are completely replaced by the nano-sized polar nanoregions, indicative of a transition to relaxor phase (Fig. 10b). Subsequently, the specimen is quenched back to room temperature, the original lamellar domains are not restored. Instead, the grains are filled with mesoscopic tweed-shaped domains (Fig. 10c) with ill-defined domain walls compared to the observation in Fig. 10a. The presence of these small, randomly oriented tweed structure suggests that the phase nature of quenched BNT-15BT-1%Ta features an intermediate state between normal and relaxor ferroelectrics. The domain structure in the aged sample is consistent with the dielectric properties including suppressed dispersion and low permittivity. In comparison, the quenched state possesses enhanced polarizability from the tweed structure, leading to higher permitivity and more dispersive dielectric response. The tweed structure, on the other hand, demonstrates that there is still a small but distinct residual macroscopic asymmetry in the quenched sample, which is also supported by the pyroelectric data in Fig. 9c. It should be noted that the polar phase metastability at room temperature is witnessed only in those compositions with $T_{\rm d}$ between 130 °C to 160 °C; too low or too high $T_{\rm d}$ gives rise to a stable relaxor or ferroelectric phase at room temperature [19,20].

4. Conclusions

Several issues related to T_d in BNT-based ferroelectrics are investigated. First one is the correlation between T_d and defect chemistry.

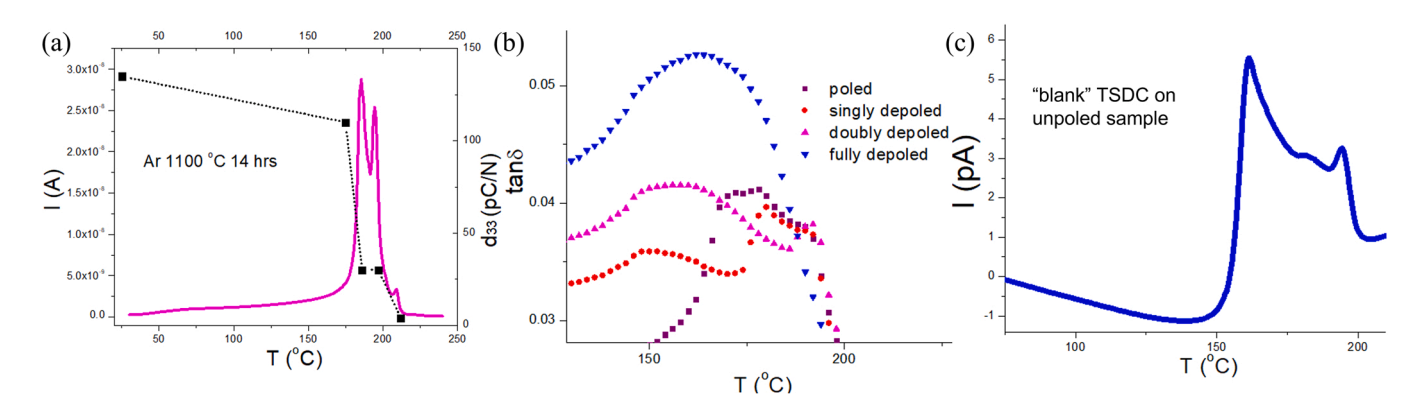


Fig. 8. (a) Pyroelectric measurement in the poled BNT-15BT-1%Ta ceramic annealed in Ar at 1100 °C for 14 hrs. (b) Temperature dependent dielectric loss to deconvolute the stepwise depolazation process in poled and partially depoled states. (c) TSDC measured in unpoled sample revealing the multiple pyroelectric peaks.

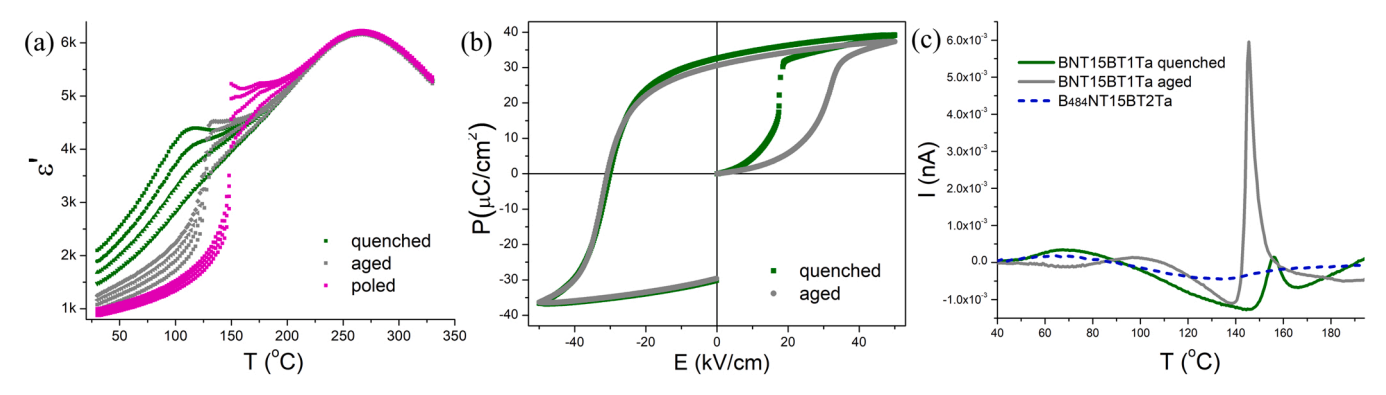


Fig. 9. (a) Dielectric permittivity measured in quenched, aged and poled states of BNT15BT-1%Ta. (b) P-E loops measured in quenched and aged states. (c) Pyroelectric measurements in quenched and aged states of BNT15BT-1%Ta, and B₄₈₄NT15BT-2%Ta as a reference.

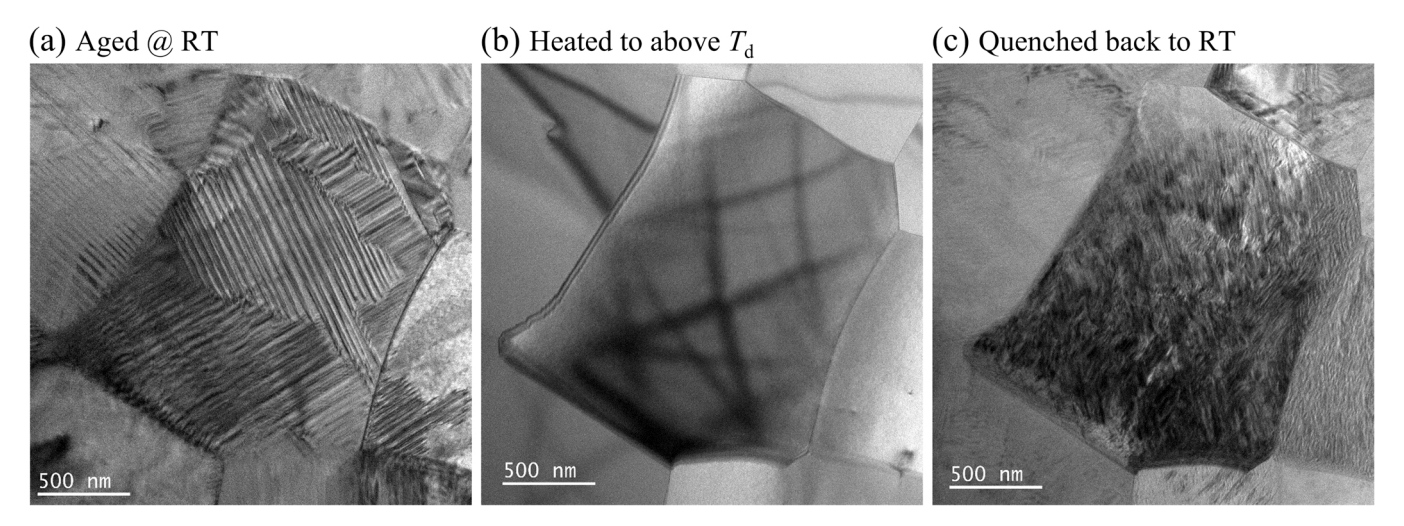


Fig. 10. (a) The coarse ferroelectric twin domains in the aged unpoled BNT15BT-1%Ta specimen at amiant temperature. (b) Polar nanoregions after heated above $T_{\rm d}$. (c) Fine tweed domains upon quenched back to room temperature.

Donor dopant decreases $T_{\rm d}$; Bi vacancy increases $T_{\rm d}$; annealing in reducing atmosphere increases $T_{\rm d}$; sintering in oxidizing atmosphere can either decrease, increase or maintain $T_{\rm d}$ depending upon the type of defects in the composition. Second one is the $T_{\rm d}$ characterization. The pyroelectric measurement can be more sensitive to the details around $T_{\rm d}$ compared to the dielectric measurement. Third one is the aging induced metastable relaxor to ferroelectric transition at room temperature taking place in some particular samples with the $T_{\rm d}$ that belongs to a certain range. The microstructural observations match qualitatively with the bulk characterizations. We hope that this work could help provide more insights into the $T_{\rm d}$ and the defect chemistry in BNT-based ferroelectric ceramics.

Declaration of Competing Interest

The authors declare that they have no known competing financial interests or personal relationships that could have appeared to influence the work reported in this paper.

Acknowledgements

This work is supported by the National Science Foundation, as part of the Center for Dielectrics and Piezoelectrics under Grant Nos. IIP-1841453 and 1841466.

References

- H.F. Kay, P. Vousden, Symmetry changes in barium titanate at low temperatures and their relation to its ferroelectric properties, Lond. Edinb. Dubl. Philos. Mag. J. Sci. 40 (1949) 1019–1040.
- [2] R. Sommer, N.K. Yushin, J.J. Van der Klink, Polar metastability and an electric-field-induced phase transition in the disordered perovskite Pb(Mg_{1/3}Nb_{2/3})O₃, Phys. Rev. B 48 (1993) 13230.
- [3] R.E. Eitel, C.A. Randall, T.R. Shrout, P.W. Rehrig, W. Hackenberger, S.E. Park, New high temperature morphotropic phase boundary piezoelectrics based on Bi(Me) O3–PbTiO3 ceramics, Jpn. J. Appl. Phys. 40 (2001) 5999.
- [4] K.H. Härdtl, R. Wernicke, Lowering the curie temperature in reduced BaTiO₃, Solid State Commun. 10 (1972) 153–157.
- [5] A. Chandrasekaran, D. Damjanovic, N. Setter, N. Marzari, Defect ordering and defect-domain-wall interactions in PbTiO₃: A first-principles study, Phys. Rev., B 88 (2013), 214116.
- [6] Z.T. Li, H. Liu, H.C. Thong, Z. Xu, M.H. Zhang, J. Yin, J.F. Li, L. Wang, J. Chen, Enhanced temperature stability and defect mechanism of BNT-based lead-free piezoceramics investigated by a quenching process, Adv. Electron. Mater. 5 (2019) 1800756
- [7] K.V. Lalitha, J. Koruza, J. Rödel, Propensity for spontaneous relaxor-ferroelectric transition in quenched (Na_{1/2}Bi_{1/2})TiO₃-BaTiO₃ compositions, Appl. Phys. Lett. 113 (2018), 252902.
- [8] F.H. Schader, Z. Wang, M. Hinterstein, J.E. Daniel, K.G. Webber, Stress-modulated relaxor-to-ferroelectric transition in lead-free (Na_{1/2}Bi_{1/2})TiO₃-BaTiO₃ ferroelectrics, Phys. Rev. B 93 (2016), 134111.
- [9] C. Ma, X. Tan, E. Dul'kin, M. Roth, Domain structure-dielectric property relationship in lead-free (1 – x)(Bi_{1/2}Na_{1/2})TiO₃ –xBaTiO₃ ceramics, J. Appl. Phys. 108 (2010), 104105.
- [10] X. Dai, Z. Xu, D. Viehland, Effects of lanthanum modification on rhombohedral Pb (Zr_{1-x}Ti_x)O₃ ceramics: Part I. Transformation from normal to relaxor ferroelectric behaviors, J. Mater. Res 11 (1996) 618–625.
- [11] G.H. Jonker, Some aspects of semiconducting barium titanate, Solid State Electron 7 (1964) 895–903.

- [12] H.M. Chan, M.P. Harmer, D.M. Smyth, Compensating defects in highly donor-doped BaTiO₃, J. Am. Ceram. Soc. 69 (1986) 507–510.
- [13] C.H. Hong, Z. Fan, X. Tan, W.S. Kang, C.W. Ahn, Y. Shin, W. Jo, Role of sodium deficiency on the relaxor properties of Bi_{1/2}Na_{1/2}TiO₃-BaTiO₃, J. Eur. Ceram. Soc. 38 (2018) 5375–5381.
- [14] M. Li, M.J. Pietrowski, R.A. De Souza, H. Zhang, I.M. Reaney, S.N. Cook, J. A. Kilner, D.C. Sinclair, A family of oxide ion conductors based on the ferroelectric perovskite Na_{0.5}Bi_{0.5}TiO₃, Nat. Mater. 13 (2014) 31–35.
- [15] Z. Fan, C.A. Randall, An overview of oxygen vacancy dynamics in (1-x)(Bi_{1/2}Na_{1/2}) TiO₃-xBaTiO₃ solid solution, J. Mater. Chem. C. 9 (2021) 10303–10308.
- [16] Y.I. Jung, S.Y. Choi, S.J.L. Kang, Effect of oxygen partial pressure on grain boundary structure and grain growth behavior in BaTiO₃, Acta Mater. 54 (2006) 2849–2855.
- [17] D.K. Khatua, A. Mishra, N. Kumar, G.D. Adhikary, U. Shankar, B. Majumdar, R. Ranjan, A coupled microstructural-structural mechanism governing thermal depolarization delay in Na_{0.5}Bi_{0.5}TiO₃-based piezoelectrics, Acta Mater. 179 (2019) 49–60.
- [18] B.L. Byer, C.B. Roundy, Pyroelectric coefficient direct measurement technique and application to a nsec response time detector, Ferroelectrics 3 (1972) 333–338.
- [19] D. Zhang, Y. Yao, M. Fang, Z. Luo, L. Zhang, L. Li, J. Cui, Z. Zhou, J. Bian, X. Ren, Y. Yang, Isothermal phase transition and the transition temperature limitation in the lead-free (1-x)Bi_{0.5}Na_{0.5}TiO₃-xBaTiO₃ system, Acta Mater. 103 (2016) 746–753.
- [20] X. Dai, Z. Xu, D. Viehland, Long-time relaxation from relaxor to normal ferroelectric states in Pb0.91La0.06(Zr0.65Ti0.35)O3, J. Am. Ceram. Soc. 79 (1996) 1957–1960.